

AD-A148 597

THE KINETICS OF ELECTRON TRANSFER REACTIONS IN AND AT
FILMS OF ELECTROACT. (U) NORTH CAROLINA UNIV AT CHAPEL
HILL DEPT OF CHEMISTRY C R LEIDNER ET AL. 26 OCT 84
F/G 7/4

1/1

UNCLASSIFIED

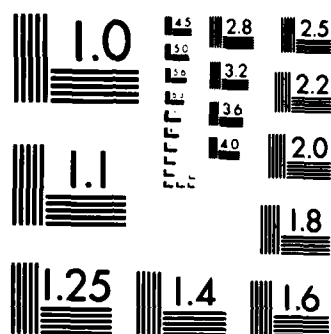
TR-9 N00014-82-K-0337

NL

END

FILED

ENC



MICROCOPY RESOLUTION TEST CHART
NATIONAL BUREAU OF STANDARDS 1963 A

AD-A148 597

OFFICE OF NAVAL RESEARCH

Contract N00014-82-K-0337

TECHNICAL REPORT # 9

THE KINETICS OF ELECTRON TRANSFER REACTIONS IN AND AT FILMS OF ELECTROACTIVE

POLYMERS

by

Royce W. Murray, Principal Investigator

Prepared for Publication

in the

Electrochemical Society

University of North Carolina
Department of Chemistry
Chapel Hill, North Carolina

October 26, 1984

Reproduction in whole or in part is permitted for any purpose of the United States Government

*This document has been approved for public release and sale; its distribution is unlimited

*This statement should also appear in Item 10 of Document Control Data - DD Form 1473. Copies of form available from cognizant contract administrator.

DTIC FILE COPY

REPORT DOCUMENTATION PAGE		READ INSTRUCTIONS BEFORE COMPLETING FORM
1. REPORT NUMBER	2. GOVT ACCESSION NO.	3. RECIPIENT'S CATALOG NUMBER
Technical Report #9		
4. TITLE (and Subtitle)	5. TYPE OF REPORT & PERIOD COVERED	
The Kinetics of Electron Transfer Reactions in and at Films of Electroactive Polymers		
6. AUTHOR(s)	7. PERFORMING ORG. REPORT NUMBER	
C.R. Leidner, R.H. Schmehl, P.C. Pickup, R.W. Murray	N00014-82-K-0337-82-K-0337	
8. PERFORMING ORGANIZATION NAME AND ADDRESS	9. PROGRAM ELEMENT, PROJECT, TASK AREA & WORK UNIT NUMBERS	
Department of Chemistry University of North Carolina Chapel Hill, NC 27514		
10. CONTROLLING OFFICE NAME AND ADDRESS	11. REPORT DATE	
Office of Naval Research Department of the Navy Arlington, Virginia 22217		
12. MONITORING AGENCY NAME & ADDRESS (if different from Controlling Office)	13. NUMBER OF PAGES	
	14. SECURITY CLASS. (of this report)	
	Unclassified	
	15. DISTRIBUTION STATEMENT (of this Report)	
	Approved for Public Release, Distribution Unlimited	
17. DISTRIBUTION STATEMENT (of the abstract entered in Block 20, if different from Report)		
S ELECTED DEC 12 1984		
18. SUPPLEMENTARY NOTES		
19. KEY WORDS (Continue on reverse side if necessary and identify by block number) electroactive polymers, electrochemistry, electron transfer kinetics, polymers, ruthenium, osmium.		
20. ABSTRACT (Continue on reverse side if necessary and identify by block number) Films of polymers and copolymers of transition metal complexes can be prepared on electrodes by reduction of vinyl substituted monomers like [Ru(bpy) ₃] ²⁺ and [Os(bpy) ₃] ²⁺ (4-pyridyl-COCH ₃ -CHPh). Using several methods, we have studied the transport of electrons through the mixed valent oxidation state of the film, and the electrocatalytic oxidation and reduction of other electroactive substances contacting the film from the solution side. The interrelationship of the rate of these processes in electrocatalytic electrode design is also discussed.		

THE KINETICS OF ELECTRON TRANSFER REACTIONS IN AND AT FILMS OF ELECTROACTIVE POLYMERS, G. R. Leisner, E. H. Schuehl, P. G. Pickup and R. W. Murray, Dept. of Chemistry, Kenan and Venable Laboratories University of North Carolina Chapel Hill, NC 27514

ABSTRACT

Films of polymers and copolymers of transition metal complexes can be prepared on electrodes by reduction of vinyl substituted monomers like $[\text{Ru}(\text{bpy})_2(\text{vpy})_2]^{2+}$ and $[\text{Os}(\text{bpy})_2(4\text{-pyridylmethyl})_2]^{2+}$. Using several methods, we have studied the transport of electrons through the mixed valent oxidation state of the films, and the electrocatalytic oxidation and reduction of other electroactive substances contacting the film from the solution side. The interrelationship of the rate of these processes in electrocatalytic electrode design is also discussed.

Over the past several years we have developed metal polypyridine complex monomers (Table I) which can be reductively electro-polymerized from acetonitrile solvent to form adherent, electroactive films on Pt and other electrodes [ref. 1,2]. The polymerization is based upon the ligand centered nature of the metal complex reduction, which activates the olefinic substituents on the various ligands toward coupling reactions. By varying the duration of the reduction procedure, relatively pinhole free polymer films containing from ca. 5 to ca. 10,000 monomolecular layers of electroactive metal complex sites can be reproducibly prepared. When placed in monomer-free $\text{Et}_4\text{NClO}_4/\text{CH}_3\text{CN}$ solution, these polymer films exhibit stable $\text{M}(\text{III}/\text{II})$ electrochemical waves at formal potentials E^0 differing according to the various metals and ligands of the monomers (Table I).

The metal complex polymer films have been attractive for further study of the polymer properties as a function of monomer unit, and of the electron transfer interactions of the polymer films with solutions of various metal complexes. The polymer films serve as membranes covering the electrode, allowing investigation of the permeability P_D [ref. 3,4] of the films to diffusion of electroactive solvents through the film to the electrode/film interface, where they are oxidized (or reduced). We have investigated the rate of electron hopping (electron diffusion coefficient D_{ct}) in the polymer films as a function of film monomer and mixed valent oxidation states, as well as developing methods for measuring D_{ct} [ref. 1,4-8].

Accession For	NTIS GRA&I DTIC TAB Unannounced Justification
By	
Distribution/	
Availability Codes	Avail and/or Special
Dist	ALL



Thirdly, we have studied the kinetics k_{12} of the electron transfer mediated oxidations of solutions of metal complexes $\text{L}_2\text{M}(\text{III})$ by the $\text{M}(\text{III})$ state of the polymer coated electrode, as a function of the electron transfer reaction free energy and of the film monomer [ref. 5,8]. Previous and newly acquired results for PD , s_{pol} , D_{ct} and k_{12} are collected and compared in this paper.

Solutions of metal poly-pyridine complexes in contact with the redox polymer film-coated electrodes exhibit a general pattern of behavior which depends on the difference in formal potentials E^0 and E^0 of the $\text{M}(\text{III}/\text{II})$ and $\text{M}(\text{III}/\text{II})$ reactions of the polymer film and solution complex, respectively. This pattern is illustrated by the montage of rotated disk voltammograms shown in Figure 1. As the potential difference $\Delta E^0 = E^0 - E^0$ is varied from negative to positive, currents are observed which are controlled by membrane permeation (very negative ΔE^0 , ---), electron diffusion in the film (negative ΔE^0 , ---), complex mass transport in the solution (ΔE^0 , the Nernst equation in a reversible wave $\Delta E^0 = 0$, -o-o-o-), and the rate of the $\text{M}(\text{III}) + \text{M}(\text{II})$ electron transfer cross reaction (positive ΔE^0 , ---). The following discussion is organized around these various classes of behavior, into which different $\text{L}_2\text{M}(\text{II})$ complexes fall according to approximate ranges or values of ΔE^0 .

Experimental details have been given elsewhere and are not repeated here [ref. 1,3-7]. Throughout, the medium is 0.1M $\text{Et}_4\text{NClO}_4/\text{CH}_3\text{CN}$ and potentials are referenced to the SCE. Film thicknesses are expressed in total electroactive $\text{M}(\text{III}/\text{II})$ sites, Γ , mol./cm², as determined by slow potential sweep cyclic voltammetry.

(---) Currents Controlled by Membrane Permeation. For very negative ΔE^0 , no electron transfer occurs between the polymer film and the solution complex. In order to oxidize the solution complex, e.g., $[\text{Ru}(\text{bpy})_2\text{Cl}]^+$ in Figure 1, it must diffuse through the polymer film in order to be oxidized at the Pt/poly- $[\text{Ru}(\text{vpy})_2]$ electrode/polymer interface. The limiting current for the rotated membrane/disk electrode voltammogram is determined by a combination of the membrane diffusion rate and mass transport in the solution, according to the equation

$$[i_{\text{lim}}]^{-1} = [d/nFAPD s_{\text{pol}} C]^{-1} + [i_{\text{lev}}]^{-1} \quad (1)$$

where i_{lev} is $0.62nFAD^{2/3} v^{-1/6} \omega^{1/2} C$ and P and D are the partition and diffusion coefficient of the solution complex

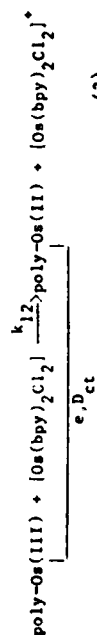
into the polymer film, respectively. The permeability P_0 of the polymer film toward $[\text{Ru}(\text{bpy})_2\text{Cl}_2]$ can be measured, from the intercepts of $(1/i)_{\text{lim}}$ plots. This has been done for a number of electroactive solutes and metal poly-pyridine polymer films. A selection of published and recent [refs. 3,4,8] results is shown in Table II.

While the permeability Table II is to date still incomplete, some useful correlations between permeability and solute or film structure can be made. First, values of permeability P_0 always fall, sensitively, into the order of neutral solute molecular size. Secondly, P_0 is depressed by increased positive charge at constant solute size; see the $[\text{Ru}(\text{bpy})_2(\text{NO})\text{Cl}]^{+}$ comparison. Somewhat surprisingly, the effect of charge seems not as large as that of size. Charge may affect P more than D . Thirdly, permeability of the poly-cationic film is very low for metal complexes which are both bulky and positively charged, e.g., $[\text{Ru}(\text{bpy})_3]^{2+}$. This is important in simplifying the mediated electron transfer or cross reaction kinetics studied at more positive potentials. All the above effects are consistent with the view [ref. 3] that the electroactive solutes dissolve in and diffuse in the film/membrane as a concentrated viscous solution, as opposed to transiting the film through pores and cracks large in comparison to molecular dimensions.

Finally, the permeabilities vary in a sensible manner with polymer structure. The polymers linked by cinnamamide chains, more lengthy than the vinyl links, are the most open structurally and are most permeable. The poly- $[\text{Os}(\text{bpy})_2(\text{vpy})_2]^{2+}$ film has the lowest permeability of all; one infers that the average monomer spacings in its structure are relatively small.

(—) Currents Controlled By Electron Diffusion Kinetics. As the potential applied to a polymer film coated electrode is made more positive, eventually potentials are reached at which significant M(III) is generated in the polymer film and begins to oxidize electroactive metal complexes in the solution contacting the film. If E_0 of the solute complex is ca. ≥ 200 -300 mV more negative than E_0 (e.g., $\Delta E < -200$ -300 mV), then this mediated oxidation begins at electrode potentials when the concentration of M(III) sites in the polymer is very small (e.g., by the Nernst equation, $[\text{M(III)}]/[\text{M(II)}] < 10^{-5}$). At the small M(III) concentration, only small $\partial[\text{M(III)}]/\partial x$ gradients can be generated in the film, and consequently the rate of M(III) site diffusion (e.g., electron diffusion) is slow and becomes the current limiting step [ref. 5]. Figure exemplifies this

situation for the mediated oxidation



where poly-Os(III) is $\text{poly-Os}(\text{bpy})_2(\text{vpy})_2^{3+}$. The region of electron diffusion control is the distinctively shaped rising part of the voltammetric wave (—) for reaction 2. The shape is determined by the manner in which the concentration M(III) depends on electrode potential, which leads to the equation:

$$i = (nFAD_{ct}^2/\sqrt{t})([\text{M(III)}]/([\text{M(III)}] + [\text{M(II)}])) \quad (3)$$

where $[\text{M(III)}]/([\text{M(III)}] + [\text{M(II)}])$ is expressed by an activity/interaction term-modified form of the Nernst equation 3. Experimental voltammograms fit equation quite well [ref. 5,8,9] and values of D can be extracted from plots of equation 3. It should be pointed out that the above discussion is based on sufficiently low film penetration or sufficiently large film thicknesses, that currents due to permeation of the electroactive complex into the film are negligible. Equation 3 implicitly includes the assumption that the mediation reaction 2 occurs at the polymer film/solution interface.

At more positive potentials on the rising (—) voltammogram, the current generated by reaction 2 (e.g., current of equation 3), can exceed i_{lev} , whereupon a limiting, mass transport controlled current i_{lev} transpires (•••••). If the electron diffusion constant of the film is sufficiently small (or the complex concentration in the solution sufficiently large), a limiting current can alternatively be reached [ref. 4,10] due to concentration polarization of M(III) sites in the film, e.g., $\partial[\text{M(III)}]/\partial x \approx -\sqrt{t}/d$. The equation for this limiting current is:

$$i_{\text{lim}} = nFAD_{ct}\sqrt{t}/d^2$$

where d is polymer film thickness.

The two electron transfer mediation based methods for

measuring D_{ct} (equation 3 and 4) are illustrated schematically in Figure 2; as are the older potential step (chronoamperometric) and sweep (cyclic voltammetric) methods [ref. 1] and a new method based on a "sandwich" electrode. In the sandwich electrode [ref. 6, 7], the added, outer porous electrode accomplishes the same act of electron donation to $M(III)$ states, that $M(II)$ complexes serve in reaction 2. The added electrode is of course a more versatile electron source, with independently adjustable potential. If the two electrode potentials of the sandwich are adjusted to yield a maximal (steady state) concentration polarization of $M(III)$ and $M(II)$ across the film, a limiting current results which is given by equation 4. Values of D_{ct} obviously can be obtained from such limiting currents.

Values of D_{ct} obtained by the various methods are shown in Table III. In view of the very different characters, presumptions, and experimental details of the D_{ct} measuring methods, the agreement between the different methods is both gratifying and significant. For instance, the agreement supports the interpretation given by equation 3 to the rising part (—) of the voltammetric wave in Figure 1.

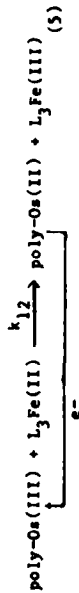
Comparing the values of $M(III/II)$ reactions in Table III is somewhat disappointing. D_{ct} for $poly-[Ru(vbp)_2]$ is appreciably smaller than the rest and that for $poly-[Os(bpy)_2(vpy)_2]$ is definitely larger. It is tempting to seek correlations in these data and of them with the permeability results. For instance, it seems logical that the polymer with the lowest permeability and the implied lowest site-site spacing might show the largest electron diffusion rate, e.g., $poly-[Os(bpy)_2(vpy)_2]$. However, there are less readily regionalized differences. D_{ct} for instance, for $poly-[Fe(vbp)_2]$ and $poly-[Ru(vbp)_2]$ fall in opposite order to the known self exchange rate constants for the soluble $[M(bpy)_3]^{2+/3+}$ complexes [ref. 11], and the more permeable cinnamide complexes transport electron as rapidly as the vbp based polymers. Given these anomalies, generalization on structural dependence of D_{ct} do not seem advisable from these data.

Table III does contain results we speculate are quite meaningful, that D_{ct} for the $poly-[Os(bpy)_2(vpy)_2]$ film increases dramatically for the more highly reduced mixed valent, electron conducting states $Os(II/I)$ and $Os(I/O)$ [ref. 9]. These states involve "bpy" molecular orbitals, and this appears to promote more rapid electron self exchange.

(-o-o-o-) Currents Characteristic Of A Reversible Wave. If

the rates of electron exchange between the $M(III/II)$ and $M(III/II)$ metal complex couples in the polymer film and solution, respectively, and the polymer film sufficiently is thin for D_{ct} is large enough) to avoid electron diffusion rate limitation, the $M(III)/M(II)$ ratio in the entire polymer film and the $M(III)/M(II)$ ratio for the complex in solution at the polymer/solution interface may remain in Nernstian equilibrium with the applied electrode potential. This case for $\Delta E^* = 0.50 - 80$ mV, exemplified by the reaction of $[Fe(bpy)_3]^{2+}$ at $poly-[Ru(vbp)_2]$ film in Figure 1, [ref. 5] gives a voltammetric wave with the classical reversible shape, just as if the solution complex were being oxidized at a naked Pt electrode. Thus, a plot of $\log i / (i_{lim} - i)$ vs E for the -o-o-o- wave in Figure 1 has a 60 mV slope [ref. 5].

(—) Currents controlled by the rate of electron transfer cross-reactions. As discussed above, where ΔE^* is negative, the rate k_{12} for $L_3M(II)$ oxidation by $M(III)$ states in the polymer film is quite large and other processes (electron diffusion, mass transport) limit the currents. If now ΔE^* is positive, the electron transfer mediation reaction is slowed and becomes current limiting [ref. 5, 8]. This is exemplified in Figure 1 by the reaction.



where L is 4,4'-dimethyl-2,2'-bipyridine and $\Delta E^* = 170$ mV. Reaction 5 proceeds in the thermodynamically unfavorable, back reaction direction, which is slower and thereby falls within a timescale which can be current-controlling. Although the equilibrium constant k_{12} of reaction 5 is only 1.3×10^{-3} , current continues to flow because the $poly-Os(III)$ state is continuously regenerated by the electrode and the oxidized complex $L_3Fe(II)$ is swept away from the polymer/solution interface.

Limiting currents (—) for reaction 5 can be analyzed for the rate constant k_{12} by plotting the equation [ref. 5, 10]

$$(6) \quad (i_{lim})^{-1} = \{nFAk_{12}[C_0]^{-1} + (i_{lev})^{-1}\}^{-1}$$

where Γ is the quantity of $poly-Os(III)$ film sites which participate in the mediation reaction 5. Since the reaction layer $\delta = PD_{0,pol}/k_{12}\Gamma$ (7)

estimated from $k_{11}f = 0.029 \text{ cm/s}$ and $\text{PD}(\text{M(bpy)}_3)^{+}$ in Table II) for penetration of $\text{L}_2\text{Fe(II)}$ into the polymer film before oxidation [ref. 10] is only ca. 0.003 \AA . It is no more than the outermost monomolecular layer of the redox polymer film, ca. $1 \times 10^{-10} \text{ mol./cm}^2$. The value of k_{11} obtained from intercepts of plots of equation 6, which is effectively the heterogeneous electron transfer rate for oxidation of $\text{L}_2\text{Fe(II)}$ at the polymer film surface, is converted to k_{12} values using this monolayer value of f . We believe this analysis is reasonable and appropriate for reaction with $k_{12} > 7 \times 10^{-6} \text{ cm/s}$ (assuming $\text{PD}(\text{M(bpy)}_3)^{+} \sim 10^{-12} \text{ cm/s}$), which corresponds to a reaction layer penetration depth of $> 1 \text{ monolayer}$, e.g., $\sim 14 \text{ \AA}$.

Similarly to the above example reaction 5, we have evaluated the mediated oxidation rate k_{12} for several series of Fe, Ru, and Os complexes with variously substituted bipyridine and phenanthroline ligands, using the three polymer films shown in Table IV. Within each series, k_{12} decrease systematically as ΔE° becomes more positive. Recognizing this, and realizing that the electron transfer reactions enjoy the simplicity of occurring at the polymer/solution interface as though the polymer surface is a "bare" electrode, we have compared the kinetic k_{12} data to the Marcus cross-reaction equation for so-called outer-sphere electron transfer reactions. This equation, written in a form suitable for comparisons to k_{12} vs ΔE° data by a linear plot even when the "q" factor is < 1 [ref. 5,8] is

$$\log k_{12} = (1/2) \log(k_{11}/k_{22}) - 8.47 \Delta E^\circ (1 + X/\Delta E^\circ) \quad (8)$$

where X is a measure of the f term and has values from 0.45 to 0.57. A summary plot of the lines best fitting the k_{12} data [ref. 5,8] according to equation 8 is shown in Figure 3. The agreement to the theoretical equation is remarkable, over a 10⁴ fold range of rate and 500 mV span of ΔE° . Note that the lines have a (pre-supposed) theoretical slope.

The intercepts of these plots, at ΔE° , yield the product $k_{11}k_{22}$ where k_{11} and k_{22} are the electron self exchange rate constants for the M(II)/M(I) and M(III)/M(II) couples. These intercept results are displayed in Table IV and are compared to the $k_{11}k_{22}$ self exchange products calculated from literature values for the M(bpy)_3^{+} (PF_6^-)_{2/3} complexes [ref. 11]. Again, the agreement of experiment with equation 8 is remarkably good, over a 100-fold range of the $k_{11}k_{22}$ product.

Comparisons between the kinetics of electron transfer reactions occurring at modified electrodes vs. occurring in homogeneous solution are an important aspects of current

electrocatalytic investigations, [10]. The data in Figure 3 represent the first comparisons of entire classes of reactions and provide in the $k_{11}k_{22}$ comparison the most extensive available example of agreement between modified electrodes and homogeneous solution kinetics. It is probable that the circumstance of little or no penetration of the solution complex into the polymer films contributed to this successful correlation. Even so, it is an interesting result, we believe, that the outermost monolayer of the polymer M(III) sites behave so ideally in spite of being embedded in a polymeric framework. Their ideal behavior, it should be noted, suggests a self exchange k_{11} rate constant (for the outermost monolayer of the polymer film) which is the same as that observed [ref. 11] in homogeneous solutions.

Acknowledgement. This research was supported by grants from the National Science Foundation and the Office of the Naval Research.

REFERENCES

1. R. D. Abruna, P. Denisevich, C. R. Leidner, T. J. Meyer and R. W. Murray, *Inorg. Chem.*, **21** (1982) 2133.
2. J. Calvert, R. R. Schuehl, R. P. Sullivan, J. S. Pacci, T. J. Meyer and R. W. Murray, *Inorg. Chem.*, in press.
3. T. Ikeda, R. R. Schuehl, R. W. Williams, P. Denisevich and R. W. Murray, *J. Am. Chem. Soc.*, **10** (1982) 2683.
4. R. R. Schuehl and R. W. Murray, *J. Electroanal. Chem.*, in press.
5. T. Ikeda, C. R. Leidner and R. W. Murray, *J. Electroanal. Chem.*, **138** (1982) 343.
6. P. G. Pickup and R. W. Murray, *J. Am. Chem. Soc.*, in press.
7. P. G. Pickup and R. W. Murray, *submitted*.
8. C. R. Leidner and R. W. Murray, *J. Physical. Chem.*, manuscript in preparation.
9. P. G. Pickup and R. W. Murray, *submitted*.
10. C. P. Andrieux, J. N. Dumas-Bouchiat and J. M. Severt, *J. Electroanal. Chem.*, **131** (1982) 1.
11. H.-S. Chen and A. C. Wahl, *J. Phys. Chem.*, **82** (1978) 2542.

TABLE II Permeability of Polymer Films

Film	Fer	$PD_s, \text{ pol. cm}^2/\text{s}^*$					RuB_3^{2+}
		RuB_2Cl_2	OsB_2Cl_2	$FeB_2(CN)_2$	$Ru(1B)_2Cl_2$	$RuB_2NOC1^{+/2+}$	
(II)	1.3×10^{-8}	1.3×10^{-9}		3.3×10^{-10}			$< 10^{-11}$
(IV)	9.2×10^{-8}	1.0×10^{-8}			7.0×10^{-10}	$5.7 \times 10^{-9}/$ 3.1×10^{-9}	
(VI)		1.2×10^{-8}	1.4×10^{-9}				1×10^{-9}
(V)			2.0×10^{-11}				$< 1.4 \times 10^{-12}$

*Calculated using C_t from measured densities [refs. 1-3] (II), (IV) and (VI), C_t for (V) by analogy with (II). Abbreviations for ligands in solution complexes are:

B = 2,2' bipyridine, 1B = 4,4' (1-propyl-OCO)₂-2,2'-bipyridine and Fer = Ferrocene

TABLE I Electropolymerized Mediators

	$E_{c,v}^0$ vs. SSCE	reference
(I) poly[Fe(vbpy) ₃] ²⁺	0.92	1
(II) poly[Ru(vbpy) ₃] ²⁺	1.14	1
(III) poly[Ru(bpy) ₂ (vpy) ₂] ²⁺	1.22	1
(IV) poly[Ru(bpy) ₂ (p-cinn) ₂] ²⁺	1.15	2
(V) poly[Os(bpy) ₂ (vpy) ₂] ²⁺	0.72	8
(VI) poly[Os(bpy) ₂ (p-cinn) ₂] ²⁺	0.65	2

bpy = 2,2'-bipyridine; vbpy = 4-vinyl, 4'-methyl-1,2, 2'-bipyridine;

p-cinn = 4-pyridyl-cinnamamide

TABLE IV Electron Transfer Rates

SERIES	$k_{11}k_{22} \text{ M}^{-2} \text{ s}^{-2} \text{ (1)}$	
	observed ⁽²⁾	calculated ⁽³⁾
(I), $\text{poly}[\text{Fe}(\text{vbpy})_3]^{3+} + \text{L}_3\text{Fe}^{2+} \xrightarrow{k_{12}}$ (3 compounds)	4×10^{12}	14×10^{12}
(II), $\text{poly}[\text{Ru}(\text{vbpy})_3]^{3+} + \text{Ru}(\text{bpy})_2\text{L}_2^{2+} \xrightarrow{k_{12}}$ (5 compounds)	64×10^{12}	69×10^{12}
(V), $\text{poly}[\text{Os}(\text{bpy})_2(\text{vpy})_2]^{3+} + \text{L}_3\text{Fe}^{2+} \xrightarrow{k_{12}}$ (10 compounds)	68×10^{12}	84×10^{12}
+ $\text{L}_3\text{Ru}^{2+} \xrightarrow{k_{12}}$ (4 compounds)	400×10^{12}	183×10^{12}
+ $\text{L}_3\text{Os}^{2+} \xrightarrow{k_{12}}$ (3 compounds)	400×10^{12}	480×10^{12}
CROSS-REACTION		$k_{12}, \text{M}^{-1} \text{ s}^{-1}$
(II), $\text{poly}[\text{Ru}(\text{vbpy})_3]^{2+} + \text{Fe}(\text{bpy})_3^{3+} \xrightarrow{k_{12}}$	observed ⁽⁴⁾ 1.2×10^6	calculated ⁽³⁾ 1.1×10^6

(1) Obtained from extrapolation of equation 8 to $\Delta E^\circ = 0$.

(2) Obtained from measured k_{12} values using $F = 10^{-10} \text{ mol/cm}^2$ [ref 5].

(3) Calculated from individual self exchange rates for $[\text{M}(\text{bpy})_3]^{2+}$ (PF_6^-)₂ in CH_3CN [ref. 11].

(4) Calculated using E and $k_{11}k_{22}$ from literature [refs. 5,11].

TABLE III Electron Diffusion

FILM	$D_{\text{ct}}, \text{cm}^2/\text{s}^*$		
	Chronoamp.	Sandwich	Mediated Oxidation
(I), $\text{poly}[\text{Fe}(\text{vbpy})_3]^{2+/3+}$	7×10^{-10}		11×10^{-10}
(II), $\text{poly}[\text{Ru}(\text{vbpy})_3]^{2+/3+}$	2×10^{-10}	14×10^{-10}	4.6×10^{-10}
(III), $\text{poly}[\text{Ru}(\text{bpy})_2(\text{vpy})_2]^{2+/3+}$	25×10^{-10}	7.5×10^{-10}	
(IV), $\text{poly}[\text{Ru}(\text{bpy})_2(\text{p-cinn})_2]^{2+/3+}$	1.2×10^{-9}		
(V), $\text{poly}[\text{Os}(\text{bpy})_2(\text{vpy})_2]^{2+/3+}$		5.4×10^{-9}	5.4×10^{-9}
$\text{poly}[\text{Os}(\text{bpy})_2(\text{vpy})_2]^{2+/+}$		2×10^{-8}	
$\text{poly}[\text{Os}(\text{bpy})_2(\text{vpy})_2]^{+/0}$		2.1×10^{-7}	
(VI), $\text{poly}[\text{Os}(\text{bpy})_2(\text{p-cinn})_2]^{2+/3+}$	9×10^{-10}	6.8×10^{-10}	
(IV), (VI) copoly $[\text{Os}, \text{Ru}(\text{bpy})_2(\text{p-cinn})_2]^{2+/3+}$	1.1×10^{-10}	$(x_{\text{Os}}=0.49)^{**}$	
	1.2×10^{-10}	$(x_{\text{Os}}=0.31)$	
	2.9×10^{-11}	$(x_{\text{Os}}=0.076)$	

* calculated with C_c values as in Table II.

** D_{ct} for Os(III/II) reaction in Os, Ru copolymer with mole fraction x_{Os} .

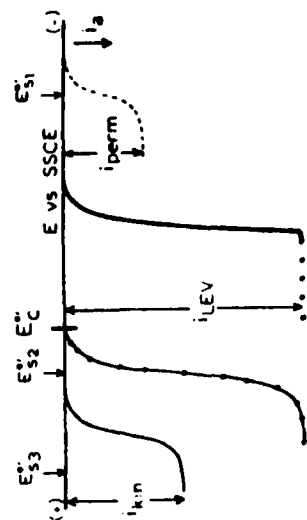


FIG. 1

	$\text{poly}[\text{Ru}(\text{bpy})_3]^{2+/3+}$ ($E^\circ = 1.18\text{V}$)	$\text{poly}[\text{Os}(\text{bpy})_3]^{2+/3+}$ ($E^\circ = 0.72\text{V}$)
permeation (O_2 , H_2O)	S1 $\text{Ru}(\text{bpy})_3^{2+/3+}$ (0.30)	$\text{Os}(\text{bpy})_3^{2+/3+}$ (0.76)
electron diffusion (O_2)	$\text{Ru}(\text{bpy})_3^{2+/3+}$	$\text{Os}(\text{bpy})_3^{2+/3+}$
mass transport (O_2)	S2 $\text{Fe}(\text{bpy})_3^{2+}$ (1.05)	
mass transport / biphenyl	S3 $\text{Ru}(\text{bpy})_3^{2+}$ (1.25)	$\text{Fe}(\text{Ru}(\text{bpy})_3)^{2+}$ (0.88)

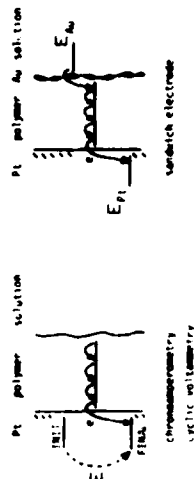


FIG. 2

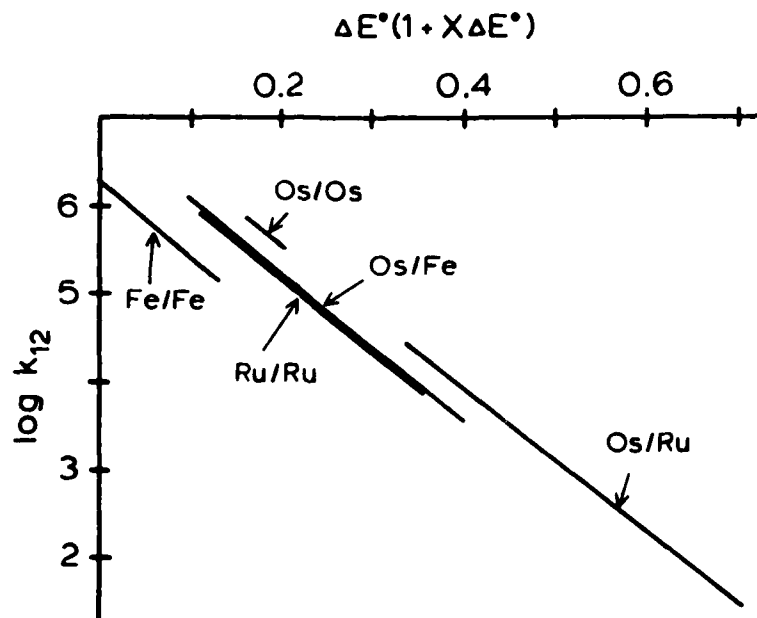


FIG. 3 Summary plot of best-fit lines to data points (not shown) as per eq. (8).

END

FILMED

1-85

DTIC